Mine Water and the Environment (2020) 39:42–56
https://doi.org/10.1007/s10230-020-00653-2

TECHNICAL ARTICLE

Beneficial Use of Deep Ordovician Limestone Water from Mine Safety Dewatering at the Xinglongzhuang Coal Mine, North China

Weichi Chen[1] · Wenping Li[1] · Wei Qiao[1] · Luanfei Li[1]

Received: 15 March 2019 / Accepted: 12 January 2020 / Published online: 16 January 2020

Abstract

The use of water from mine dewatering has become increasingly important issue in northern China. Much of this water is discharged to the environment, which wastes a valuable resource and pollutes the ecosystem. To help address this, a feasibility analysis was carried on using deep Ordovician limestone water from dewatering at the Xinglongzhuang coal mine. First, a safe hydraulic pressure was estimated using the conventional water inrush coefficient method. Then, based on the results of a water release test (drilled into an artesian aquifer), a model representing the geology and hydrology of the study area was subsequently established and calibrated to existing conditions and water release test results, using the numerical simulation program FEFLOW. Finally, according to a contract signed between the mine and a local industrial water consumer, two cases of dewatering were discussed using the model to maintain a balance between mining safety and supplying water for nearby industrial operations. During the calibration and prediction analysis, the permeable faults were identified as the most important factor in water management and a key factor for balancing the aforementioned needs.

Keyword Feasibility analysis · Water release test · FEFLOW · Numerical simulation

Introduction

Water is a vital resource and there is a severe shortage of it on the global scale (Afzal et al. 2016; Islam et al. 2017; Kotir et al. 2016). This issue is particularly acute in China, where it is estimated that only 2200 m^3 of water is available per capita, compared to the global average of 8800 m^3 (Huo et al. 2016; Sun et al. 2017). Excessive exploitation of shallow groundwater has aggravated this shortage and has triggered various environmental issues and geological hazards, such as land subsidence, seawater intrusion, and water quality deterioration (Mahmoudpour et al. 2016; Motagh et al. 2017). Land subsidence occurs often in northern China (Huang et al. 2014; Wang et al. 2014), so the sustainable use of water resources deserves more attention there.

North China has abundant coal reserves and a number of coal mines, most of which are threatened by floor water inrush from confined Ordovician limestone aquifers (OLA) (Sun et al. 2016; Zhang 2005) located beneath the mineable Permo-Carboniferous coal seams. The OLA are an abundant water resource, but are also a major mining hazard due to frequent mine water inrush events that have caused heavy casualties and economic loss (Yin et al. 2018). There are two main reasons for such mining accidents. First, the water pressure in the OLA is high, and there is limited thickness of aquitards between mine voids and the aquifers. Protection provided by the aquitard layers can be easily overcome, allowing water to flow into the working faces (Yin et al. 2015). Second, significant discontinuities, including permeable faults, exist in the aquitards and floor rocks, which increases the potential for an outburst by forming inrush channels and decreasing the mechanical resistance of the floor rock (Li et al. 2011; Zhang et al. 2014; Zhu and Wei 2011).

Additionally, the subsequent management and use of discharged mine water has received little attention, especially for deep OLA water (Wu et al. 2006, 2010). The discharge of raw mine water has wasted water resources

Electronic supplementary material The online version of this article (https://doi.org/10.1007/s10230-020-00653-2) contains supplementary material, which is available to authorized users.

✉ Wenping Li
Wpli1965@163.com

[1] Institute of Mine Water Hazards Prevention and Controlling Technology, School of Resources and Geosciences, China University of Mining and Technology, Xuzhou 221116, Jiangsu, China

and contaminated surface water systems (Abraham and Susan 2017; Li and Zhou 2006; Singh et al. 2017). Therefore, the feasibility of using OLA water in other nearby industrial facilities was analyzed to simultaneously alleviate the water shortage in northern China and promote safe coal mining.

The Xinglongzhuang coal mine (XCM) was used as a case study. First, a safe value of dewatering to reduce hydraulic pressure was determined and a target drawdown of the OLA were calculated by conventional formula. A multi-hole water drawdown test was performed, using free flowing artesian wells, to provide data for numerical modeling. Then, a numerical simulation model was established and calibrated to the results of the dewatering test using FEFLOW. Finally, two cases of dewatering were considered to achieve a balance between safe mining and providing a reasonable water supply for the other industrial user. An interesting discovery was that the permeable faults, traditionally viewed as a threat to mining, were identified as a feature that could be used to facilitate water recovery.

Study Area

Dilemma of Mine Water as a Resource

The XCM is located in southeastern Yanzhou, a county in Jining City of Shandong Province, China (Fig. 1). The area of the mine is 57.7 km^2, with a length of 13.1 km along its strike and a width of 6.8 km. The study area is an alluvial plain, which gradually decreases in elevation from northeast to southwest with the elevation ranging from 52 to 44 m above sea level. The elevation of the industrial square is 49 m, and is generally not threatened by flooding except for severe events. The mine is dominated by a semi-humid monsoon climate with four distinct seasons, which is a transitional climate between the mainland and the ocean. The annual average rainfall is 706 mm while the evaporation capacity is 1780 mm and the rainy season is concentrated in July to August. The proven reserve is 3.73 billion metric tons (t), of which 2.35 billion t is minable. The current production capability of the mine has reached 190 thousand t per day. However, with the increased scale of exploitation, local conflicts on water use are intensifying. For example, extraction of water for both domestic and industrial water has resulted

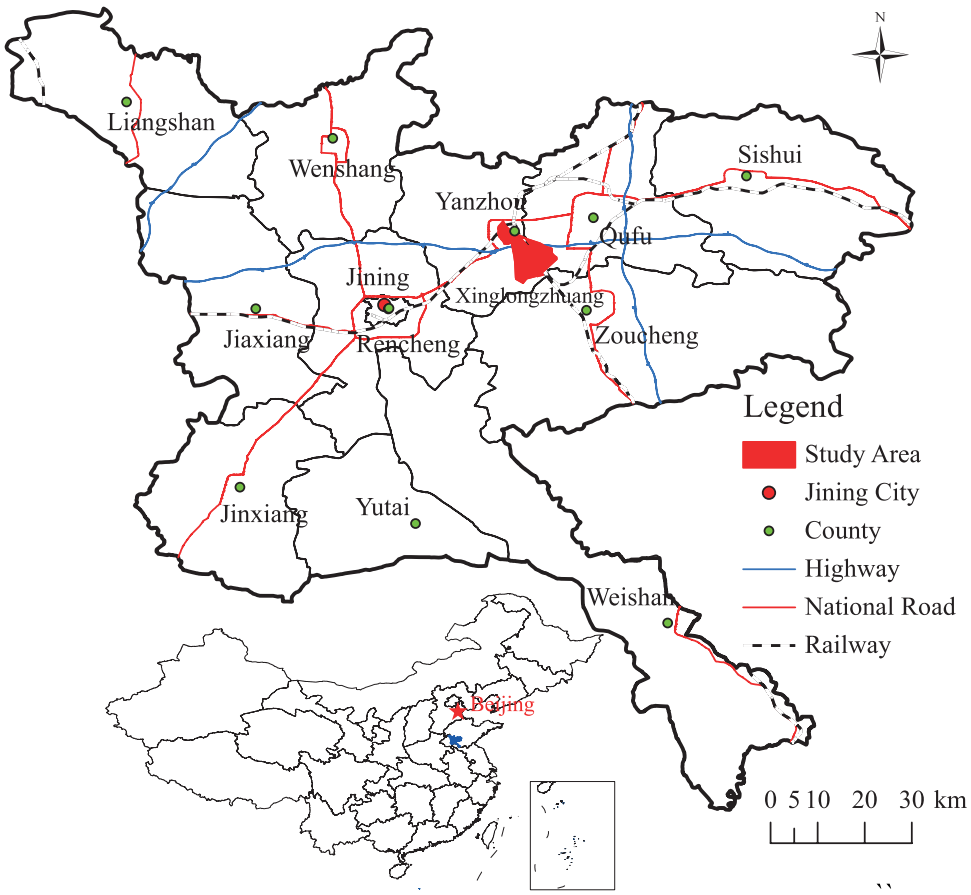

Fig. 1 Location of XCM

in uneven subsidence and is a potential threat to the stability of shaft linings at XCM. Domestic and industrial water use also negatively impacts the availability of agricultural water and the health of the environment. On the other hand, to prevent hazards of floor water inrush, a large amount of water from OLA is discharged to the surface environment. Such discharge not only heavily contaminates the surface water system but also wastes a valuable resource. Feasible solutions are needed to resolve these conflicts.

Geology and Hydrogeology

The primary strata in the XCM, from the top down, consist of the Quaternary sediments, Jurassic sandstone, Permian, Carboniferous mudstone, and Ordovician limestone. The minable coal seams are the Carboniferous Taiyuan formation no. 16 and 17 coal seams (hereafter referred to as the lower coal group), with an average thickness of 1.2 and 0.9 m, respectively. The main aquifers are the Quaternary pore aquifer, upper Jurassic sandstone aquifer, sandstone aquifer of the Permian Shanxi formation, Carboniferous thin layer limestone aquifer, and the OLA. In contrast to the other aquifers, the upper Quaternary sand layer has abundant water and rich recharge, but it does not pose a hazard to mining because of the large vertical interval between this upper aquifer and the mine workings. As shown in Fig. 2, the main aquifers of concern are the no. 13 and 14 limestone aquifers in the Carboniferous Benxi formation and the OLA. The thickness of the no. 13 limestones aquifer is 0–10 m (averaging 7 m), and the distance to the lower coal group is 10–44 m (an average of 22 m). With a unit water inflow of 0.02 L/s m and a permeability coefficient of 0.3 m/day, this aquifer was defined as a weak water-bearing aquifer. The no. 14 limestone aquifer is 0–11 m thick (averaging 3.2 m), and it is 21–51 m (averaging 36 m) from the lower coal group. This aquifer, with a unit water inflow of 0.0032 L/s m and a permeability coefficient of 0.02 m/day, was also defined as a weak water-bearing aquifer. The interval between the no. 13 and 14 limestones aquifers and the OLA is 15 and 7 m, respectively. The OLA mainly consists of gray-white to turquoise limestone which is massive, dense, pure, and brittle, with a thin gray-green mudstone layer at the top. The OLA has a unit water inflow 0.0022–1.29 L/s m, and a permeability coefficient of 0.0043–2.31 m/day, and it is defined as a confined aquifer with dominant fracture flow, relatively developed karstic voids, and strong water-bearing capacity. The water yield of the drill holes ranges from 8 to 126 m^3/h (an average of 61 m^3/h). The interval between OLA and the lower coal group is 25–67 m (an average of 46 m). The OLA has the greatest influence on the lower coal group due to its thickness (over 100 m) and hydraulic pressure, ranging from 3.5 to 12.0 MPa (Ji et al. 2003; Ma and Zhong 2011; Zhang et al. 2015). Therefore, the OLA is the main target investigated in this paper.

Faults and Fissures

The XCM belongs to the Yanzhou coalfield, where the folds and faults are well developed due to Indonesian, Yanshanian, and Himalayan plate movements (see Supplemental Fig. 1). The XCM is adjacent to the Dongtan and Baodian coal mines, and the area is impacted by the Ziyang and Puzi faults to the east and west. The XCM geology is defined as a monoclinic structure with an uneven distribution of faults. There are more faults between the main Ziyang and Puzi faults than in other areas.

Many field tests including seismic surveys and hydrochemical connectivity tests have shown that these faults differ in permeability. The Puzi fault has a high permeability, especially the Puzi no. 1 and 2 faults, while the Ziyang fault has very low permeability, as proven by core drilling investigations. The permeable faults not only connect other aquifers but also likely increase the risk of karst pillar collapse, increasing the potential for water inrush (Bai et al. 2013; Li et al. 2017; Ma et al. 2016).

Methods

Dewatering Pressure for Safe Mining

If the aquifer hydraulic pressure is extremely high while the cumulative thickness of aquitards between the aquifer and the mining void is low, pressurized OLA water will crush the protective strata and flow into working faces with potentially catastrophic consequences. Thus, the water inrush coefficient (T_s), defined as the maximum water pressure sustained by unit strata under safe conditions, was proposed by Jiaozuo Ming Water Control in 1964 (Liu 2009). T_s (MPa/m) can be calculated as follows:

$$T_s = \frac{P}{M} \tag{1}$$

where P is the hydraulic pressure of the confined aquifers below the seam floor (MPa), and M is the cumulative thickness of aquitards between the roof of the confined aquifers and the seam floor (m). In addition, according to SACMSC (2018), the critical water inrush coefficients as 0.1 and 0.06 MPa/m for normal and complex geological conditions, respectively. A safe value of T_s of 0.1 MPa/m was also reported by Qiao et al. (2014) for the Dongtan coal mine adjacent to the XCM, and so was adopted as a safe dewatering pressure in this study.

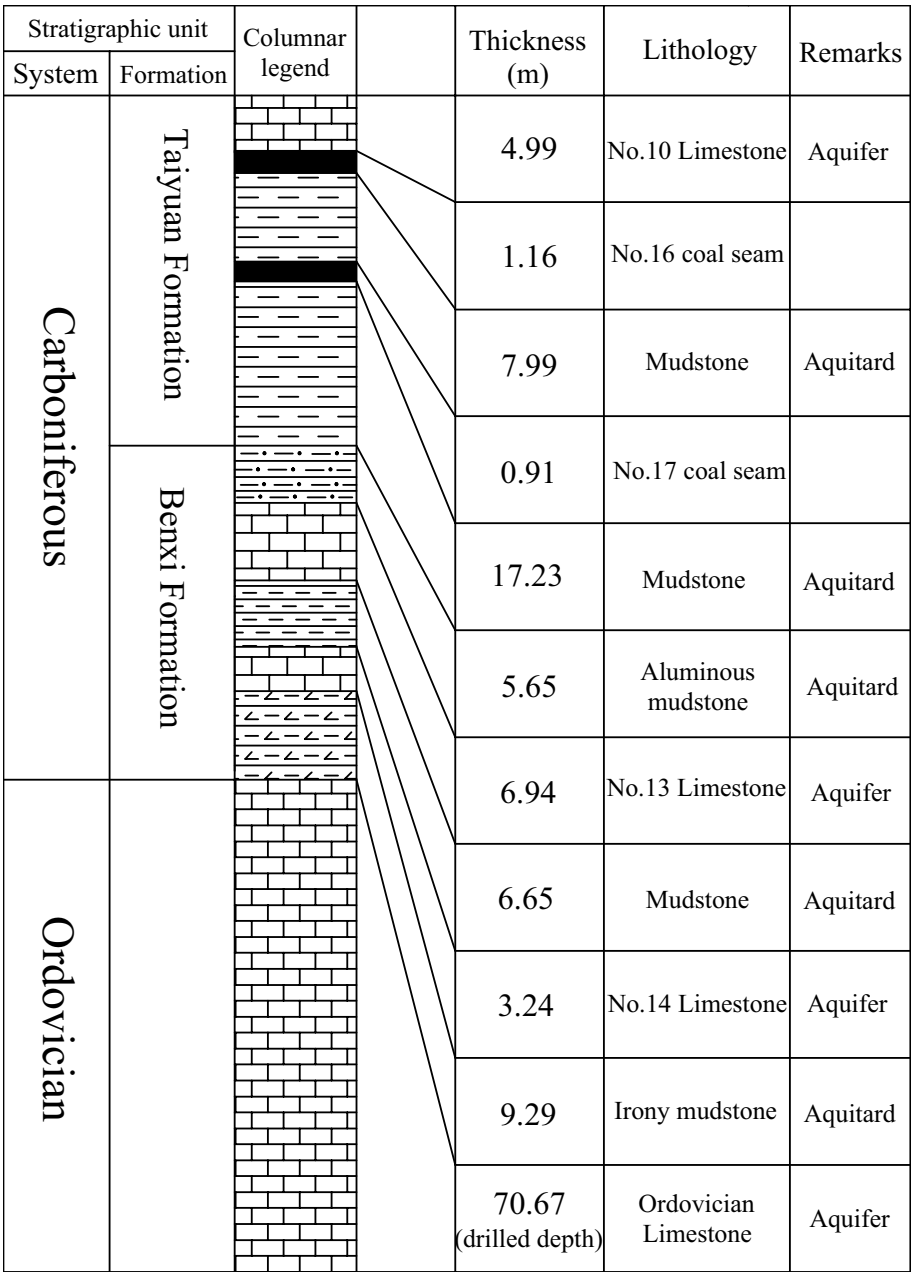

Fig. 2 Stratigraphic column of XCM

Safe mining involves other issues such as managing the mine pressure and gas explosions, but dewatering is a mandatory requirement in China and must be done safely. The calculated unmitigated T_s of OLA for the lower coal group is 0.08–0.20 MPa/m (Supplemental Fig. 2. Hence, it is essential to decrease it to a safe value.

Cooperation in Water Supply

Of the chemical plants nearby, the Guohong Coal Chemical Enterprise (GCCE) has the highest demand for water. It is a large coal chemical enterprise producing alcohol esters from high-sulfur coal and is located about 15 km away from the XCM. According to GCCE's project construction plan, the company will produce 500,000 t of methanol annually in the first phase and 1,000,000 t in the second phase, requiring at least 29,000 m^3/day of industrial water. The radius of depression cones shaped by this extraction from phreatic aquifers extends over 20 km from the factory, and the resulting compression of soil layers has caused slight infrastructure deformation.

Analysis of the major ions in the water from the OLA being discharged by the XCM confirmed that the water meets the standards for industrial use (Ministry of Health 2005). The water chemistry type is mainly SO_4^{2-}, Ca^{2+}, and Mg^{2+}; and the total dissolved solids (TDS) is less than

1000 mg/L, with a pH ranging from 7.0 to 7.3. Therefore, there is a potential opportunity for cooperation between the XMC and GCCE (referring to Supplemental Table 1): after simple treatment, the discharged mine water could be used directly by GCCE. However, the suggestion of further study of other water quality parameters to reduce potential negative effects to industrial progress was proposed. Preliminary cooperation on the mine water supply was established between the XCM and GCCE under the leadership of the Jining municipal government. The XCM is required to construct a water pipe of 16.5 km to deliver the mine water, while GCEE will take charge of its routine maintenance. The Jining municipal government helped expropriate land for the pipeline, and the two companies shared expenses. Furthermore, the contract stipulated a total supplied water volume between 29,000 and 34,000 m^3/day, including water loss in delivery and a reserve water sump.

Multi-hole Water Release Test of OLA

A supplementary hydrogeological investigation was performed to examine the water abundance characteristics of the OLA. The investigation included 33 drilled holes: 7 holes in the no. 13 limestone aquifer, 3 holes in the no. 14 limestone aquifer, and 23 holes in the OLA. There were 15 surface drillings and 8 subsurface drillings from the coal mining roadway; surface and subsurface holes are prefixed with "O2-" and "FO2-", respectively. The subsurface drill holes are also termed artesian wells since they encounter the deep high-pressure water of the OLA. Three of the subsurface drillings (FO2-8, FO2-12, and FO2-18) were chosen to act as water release holes. The other drill holes were used as observation holes. The layout of the water release test is shown in Fig. 3. In the 48 h between 23:00 in March 24 and 23:00 on March 26, 2017, the total discharged amount of water was 8424 m^3. Subsequently, the valves of the artesian wells were shut down to allow the water table to recover for another 48 h, until 23:00 in March 28, 2017. The stable water release flow from FO2-8, FO2-12, and FO2-18 holes was 37, 77, and 60 m^3/h, respectively. During the water release and recovery experiments, the water level of the surface holes and subsurface holes were observed synchronously and the observation frequency was carried out according to the requirements of unstable flow pump tests (see Supplemental Table 2). When the water release was finished, the surrounding area of release water holes FO2-8, FO2-12, and FO2-18 formed a stable cone of depression, and the surface holes O2-18 and subsurface holes FO2-3a reached maximum drawdowns of 3.89 and 6.12 m, respectively. The distance (calculated by the orifice coordinates) between O2-18 and FO2-8 is 797 m, and FO2-18 is 1140 m, and the distance between FO2-3a and FO2-8 is merely 142 m, indicating, as expected, that the smaller the distance from the release hole, the greater the water level drawdown within the Ordovician limestone confined aquifers (OLA). The water level decrease of observation holes of no. 13 and 14 limestones aquifers also were monitored: 4.08 m (L13-5), 2.04 m (L14-4), 1.82 m (L14-16), 2.54 m (L13-8), 2.33 m (L13-7), 2.07 m (L13-3), 1.41 m (L13-2), 0.73 m (L13-1), and 0.29 m (L13-4). Additionally, when the artesian well valves were shut down, the water level in all holes increased continuously. This indicates a hydraulic connection between OLA and the no. 13 and 14 limestones aquifers through the pervious faults (Ji et al. 2003).

Numerical Model

Based on the regional, geological, and hydrogeological background provided above, the northern and western boundaries of the model area were taken as the Ziyang fault and Puzi fault, which were treated as impervious and permeable boundaries, respectively. The eastern and southern boundaries were the Baodian and Dongtan coal mines, which were generalized as flow boundaries. Vertically, the model consists of 10 strata, where the top layer is the no. 16 coal seam (1.16 m thick) and the bottom layer is the OLA (100 m thick). Due to intense tectonism, the OLA shows significant spatial variation in its hydrogeological parameters. So, it was depicted as a heterogeneous and anisotropic aquifer, while the no. 13 and 14 limestones were both modeled as homogeneous and anisotropic aquifers. Because all the aquifers and aquitards are penetrated by faults, water can flow between the OLA and no. 13 and 14 limestones. The groundwater model is governed by the following partial differential equations representing a multi-layered confined groundwater system.

$$
\begin{aligned}
&\frac{\partial}{\partial x}(k_1\frac{\partial H_1}{\partial x})+\frac{\partial}{\partial y}(k_1\frac{\partial H_1}{\partial y})+\frac{\partial}{\partial z}(k_1\frac{\partial H_1}{\partial z})+v_1=S_{s1}\frac{\partial H_1}{\partial t}(x,y,z)\in w_1\\
&\frac{\partial}{\partial x}(k_2\frac{\partial H_2}{\partial x})+\frac{\partial}{\partial y}(k_2\frac{\partial H_2}{\partial y})+\frac{\partial}{\partial z}(k_2\frac{\partial H_2}{\partial z})+v_2=S_{s2}\frac{\partial H_2}{\partial t}(x,y,z)\in w_2\\
&\frac{\partial}{\partial x}(k_{3x}\frac{\partial H_3}{\partial x})+\frac{\partial}{\partial y}(k_{3y}\frac{\partial H_3}{\partial y})+\frac{\partial}{\partial z}(k_{3z}\frac{\partial H_3}{\partial z})+v_3=S_{s3}\frac{\partial H_3}{\partial t}(x,y,z)\in w_3\\
&v_1=k_4\frac{H_3-H_1}{M};v_2=k_4\frac{H_3-H_2}{M};v_3=v_1+v_2\\
&H_1(x,y,z,t)|_{t=0}=H_{1,0}(x,y,z);H_2(x,y,z,t)|_{t=0}=H_{2,0}(x,y,z)\\
&H_3(x,y,z,t)|_{t=0}=H_{3,0}(x,y,z)\\
&T\frac{\partial h}{\partial n}\Big|_{\Gamma_1}=q(x,y,t)(x,y)\in\Gamma_1,t\geq 0;T\frac{\partial h}{\partial n}\Big|_{\Gamma 2}=0(x,y)\in\Gamma_2,t\geq 0
\end{aligned}
\tag{2}
$$

where: w_1, w_2, and w_3 are the domains of the no. 13 limestone aquifer, no. 14 limestone aquifer, and the OLA, respectively; k_1, k_2, and k_3 are their hydraulic conductivity (m/day); S_{s1}, S_{s2}, and S_{s3} are their specific storage (m^{-1}); k_x, k_y, and k_z are the hydraulic conductivity of the OLA in the x, y, and z directions (m/day); v_1, v_2, and v_3 are respectively the

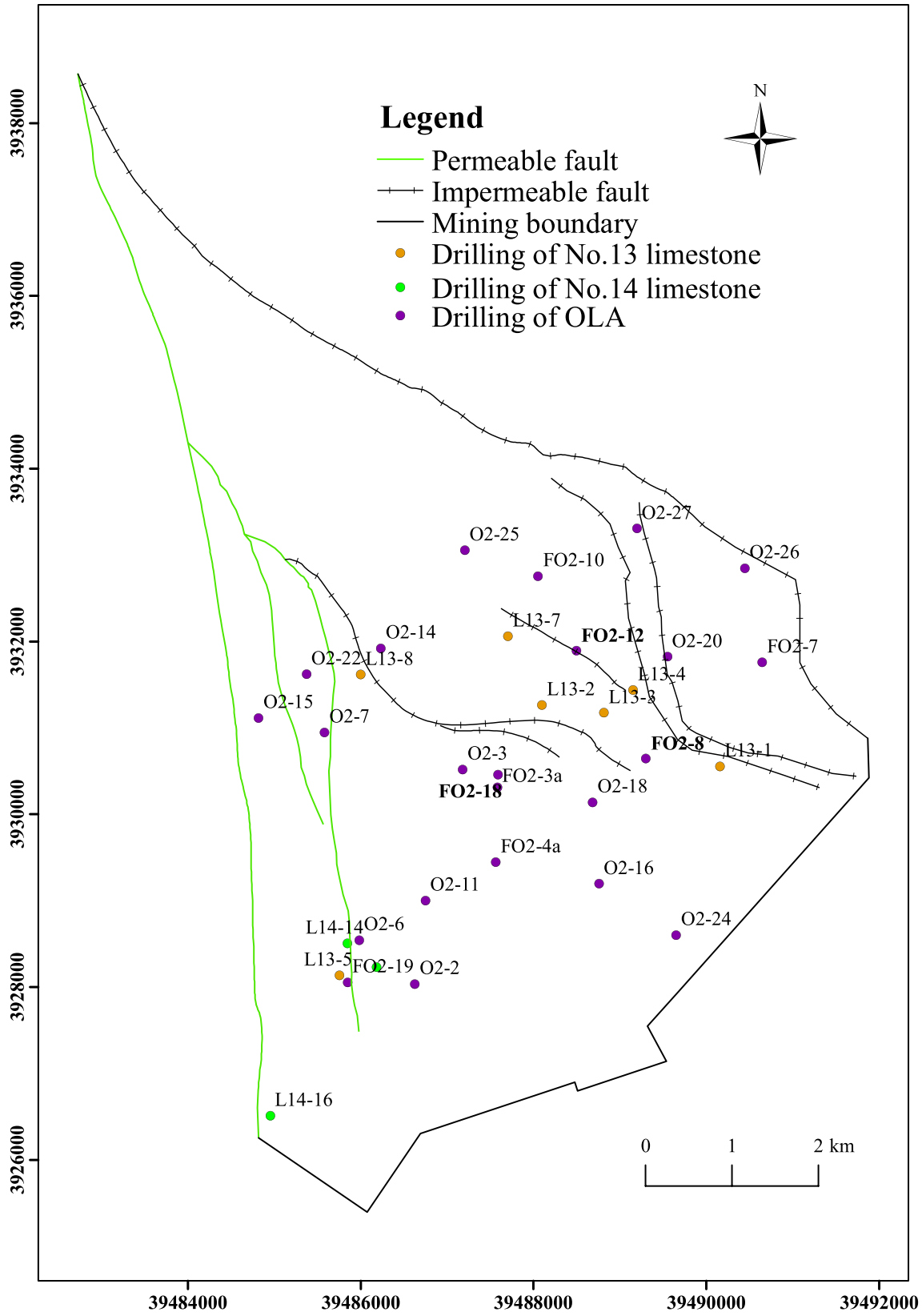

Fig. 3 Layout of the water release test

recharge flow velocities between the no. 13 limestone and the OLA, between the no. 14 limestone and the OLA, and of OLA accepting other aquifers (m/day); k_4 is the flow velocity of permeable faults (m/day); M is the equivalent seepage thickness of faults (m); H_1, H_2, and H_3 are the water table (m) for the three aquifers; $H_{1,0}$, $H_{2,0}$, and $H_{3,0}$ are the initial water table (m); Γ_1 is the impervious boundary; and Γ_2 is the fluid-flux boundary.

The Equations in (2) are too complex to be solved by traditional analytic methods. But an analysis can be done using simulation software such as FEFLOW (Mu et al. 2018) in a numerical code based on the finite element method (FEM). Consequently, a three-dimensional model involving the coal seams, aquifers, aquitards, and faults was established. The model consisted of 10 layers containing 115,400 elements and 66,567 nodes (Fig. 4).

Results

Parameter Zoning

The hydrogeological parameters of the OLA were calculated using traditional graphical methods (Cooper and Jacob 1946; Theis 1935) according to water level monitoring data from the drill holes of the water release test (referring to Supplemental Table 3). The results indicated obvious parameter zoning of the OLA, which also showed that it is reasonable to treat the OLA as a heterogeneous and anisotropic aquifer. On this basis, the OLA was divided into 12 zones with the estimated initial specific storage and conductivity using the drill hole data located in each unit (Fig. 5). Zone unit no. 1 contains no drill holes but is too large to be merged into the other units. Its initial hydrogeological parameters were therefore assigned by referring to adjacent units.

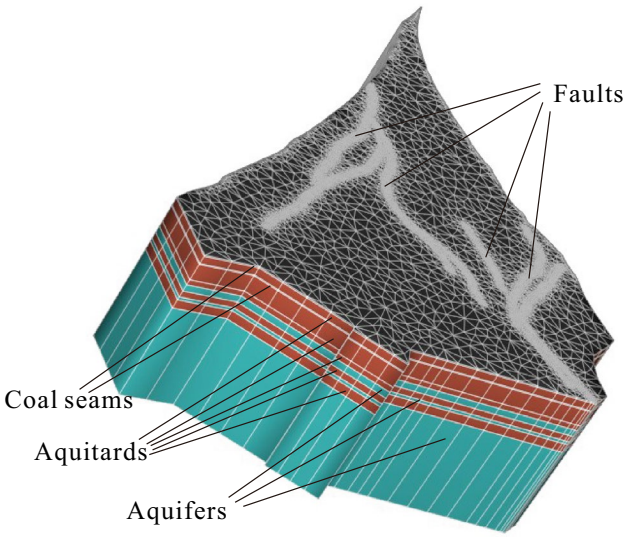

Fig. 4 Three-dimensional (3D) model

Fracture structures and faults can be depicted explicitly by the numerical model; however, hydrogeological testing has not yet been conducted in the faults. Initial parameters for the faults were assumed and then subsequently modified as part of the model calibration process. Before running the simulation, the model was run with steady state flow (natural condition) to obtain improved input parameters. Many reported models for the area have not included this step (Dong et al. 2012; Mu et al. 2018). A comparison of the initial flow field between kriging interpolation of the observed values and those calculated in the model run is shown in Supplemental Fig. 3. Data from 23:00 March 24, 2017 to 23:00 March 28, 2017 were fitted for model calibration. After hundreds of trial model runs and correcting the parameters, fitted hydrogeological parameters were obtained (Table 1); the final permeability of faults equaled 18 m/day.

Calibration and Validation

The calibration and validation steps can help the user understand the error distribution and sensitivity level of the program, and determine whether the fitted model could be applied as a predictive tool. By varying selected parameters and re-running the program, the calculated water level can be calibrated. The outputs at termination of the model runs were compared with the observed hydraulic head of each hole (referring to Supplemental Table 4). Although the relative errors between calculated and observed values were small (the maximum was 5.97% for the O2-2 hole), an analysis of the dynamic change of water head is also essential. Dynamic changes in water levels for some representative drill holes were modelled to illustrate the simulation effect, in which the time-based water head change was examined in short time steps.

Then, the observed and calculated flow fields at termination were compared (Supplemental Fig. 5). The calculated groundwater field was generally consistent with the measured one. Some partial inconsistency may have been caused by the subjectivity of the operators, the complex hydrogeology, and software limitations. This was further researched below.

Sensitivity Analysis

Successful calibration and validation indicated that the model could reproduce the water release data numerically with satisfactory accuracy. Nevertheless, remaining uncertainty could lead to unacceptable risks for engineering applications. Sensitivity analysis helped identify the dependence of the outputs on various input factors. Then, the most

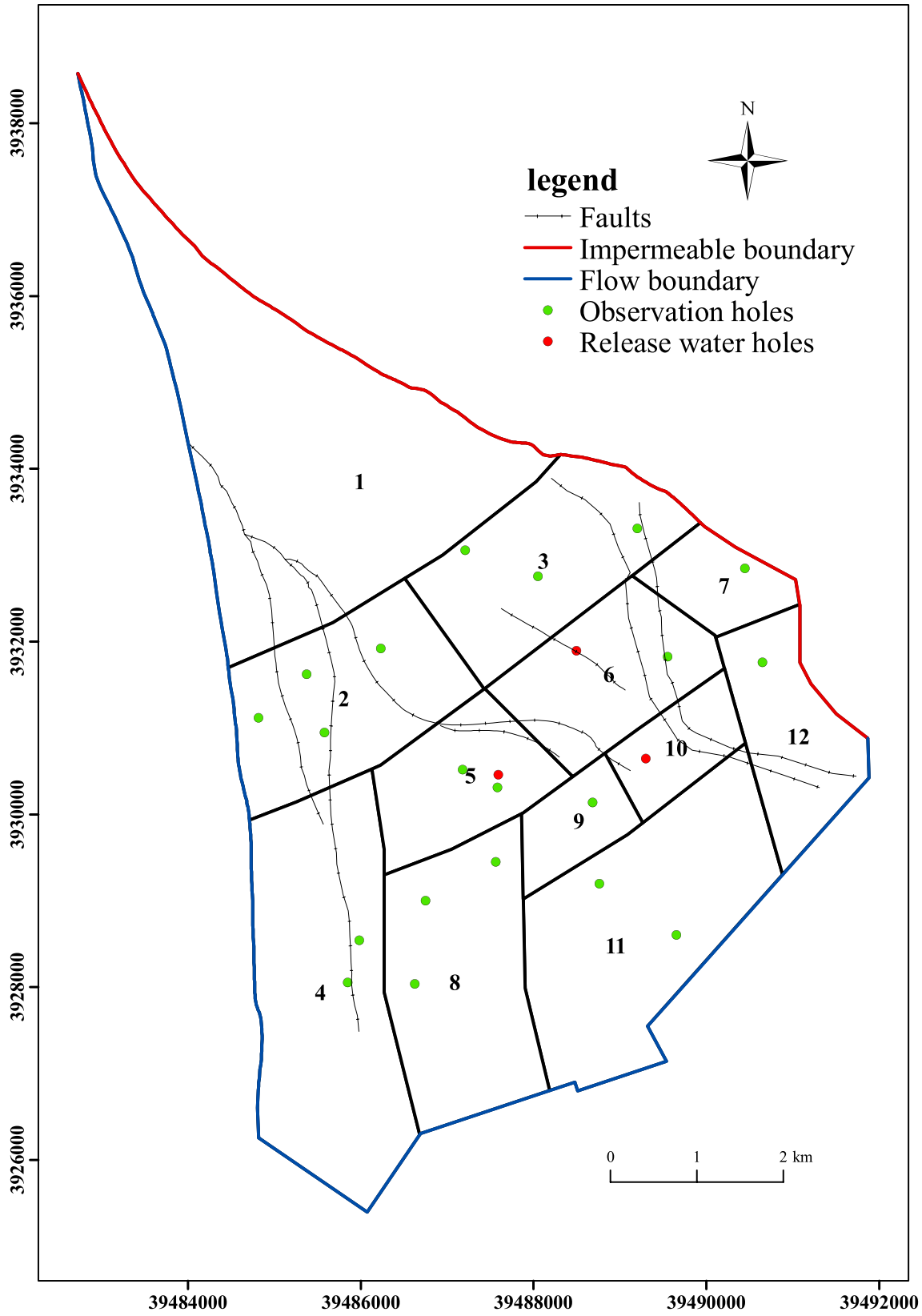

Fig. 5 Parameter zoning of the numerical simulation

Table 1 Numerical solution of parameter zoning for OLA

Unit	K_x (m/day)	K_y (m/day)	K_z (m/day)	S_s ($\times 10^{-6}$ m^{-1})	Unit	K_x (m/day)	K_y (m/day)	K_z (m/day)	Ss ($\times 10^{-6}$ m^{-1})
1	10.1	9.8	3.3	1.2	7	3.7	4.1	0.8	3.9
2	19.5	20.2	5.2	2.9	8	9.1	10.1	2.8	4.4
3	14.8	15.7	4.4	8.2	9	2.2	2.5	0.8	2.2
4	5.8	6.1	2.5	4.4	10	1.8	2.1	0.5	3.1
5	16.8	15.4	2.8	1.4	11	0.8	0.8	0.2	8.4
6	6.1	6.2	1.1	5.3	12	1.1	1.4	0.4	1.6

sensitive factor was used to predict possible risks in the future. The main factors in the model, namely the permeability of faults (k_f), the horizontal and vertical conductivity of OLA (k_h and k_v), and the specific storage of OLA (S_s) were selected for analysis (ElZehairy et al. 2018). The relative water level changes in the observation holes were defined as the sensitivity criterion, while each factor was increased or decreased by 10% and 20% (Xue et al. 2018). A total of 13 observation holes were selected to test the sensitivity, including 11 OLA holes representing each unit, the L13-4 hole in the no. 13 limestone, and the L14-4 hole in the no. 14 limestone (Fig. 6). Surprisingly, although the OLA was the target aquifer in this paper, the change of water table was larger for k_f, indicating that k_f is more sensitive than k_h, k_v, and S_s, especially for drill holes near the permeable faults such as O2-2 and O2-6 (Fig. 6d). The sensitivity of the results to k_v is higher than to k_h, suggesting that a change in vertical conductivity may induce a longer seepage path than that in the horizontal direction (Fig. 6a, b) (Wu et al. 2016). The sensitivity of S_s was the lowest among the four main factors. Therefore, the permeability of the OLA is high and its lateral recharge may be more significant than the static reserves.

Feasible Utilization of OLA Water

According to the contract, the total volume of water to be supplied to GCCE ranges from 29,000 to 34,000 m^3/day. So, two cases of dewatering were considered. In Case 1 (the regional dewatering plan), the water level of the whole OLA was dropped simultaneously. However, this caused a large amount of mine water to be released, exceeding the consumption capability of the GCCE. In Case 2 (the local dewatering plan), the OLA was divided into three zones based on the hydrogeology, and the mine water was released successively.

Case 1

Five additional subsurface drill holes were completed to assess the regional dewatering plan. The target drawdown can be calculated by inversely solving Eq. (1). This target drawdown was assigned as a constrained head condition in FEFLOW. The commands can direct the program to release water until the water level of subsurface drillings were dropped to the target value, meanwhile the volume and time of dewatering were recorded automatically. This is a user-friendly feature in FEFLOW. The *Ts* distribution of case 1 is shown in Fig. 7, and the corresponding volume and time are shown in Table 2. Although this reduced the T_s to a safe value for most of the domain, the total water inflow reached 59,468 m^3/day, including 7538 m^3 that was recharged from the no. 13 and 14 limestone aquifers due to the faults. Thus, excess mine water was produced in this case. In addition, the time to reach target T_s was so long that it overstepped the mining schedule significantly. Thus, a local dewatering plan was proposed (case 2).

Case 2

Due to the excess water release and long dewatering time in case 1, case 2 included some adjustments. The results of case 1 indicate that subsurface drillings near the permeable faults (FO2-19 hole) have larger water volume and longer dewatering time than the other drill holes. Besides, in case 1, the assignment of water release holes produced little pressure response for the no. 1 unit because there were no drill holes in it. In case 2, the domain of OLA was divided into three zones based on the hydrogeology and fracture/fault features, while some proposed drill holes were included in the model to accelerate the dewatering (Fig. 8a). The function of constrained water head was used again. The distributions of T_s from the local dewatering are shown in Fig. 8b–d, which correspond to stage 1, 2, and 3 (Table 3), respectively. In stage 1, after dewatering for 44 days, a stable water amount of 29,119 m^3/day can be supplied by 5 proposed holes. In stage 2, after dewatering for 36 days, 29,159 m^3/day can be

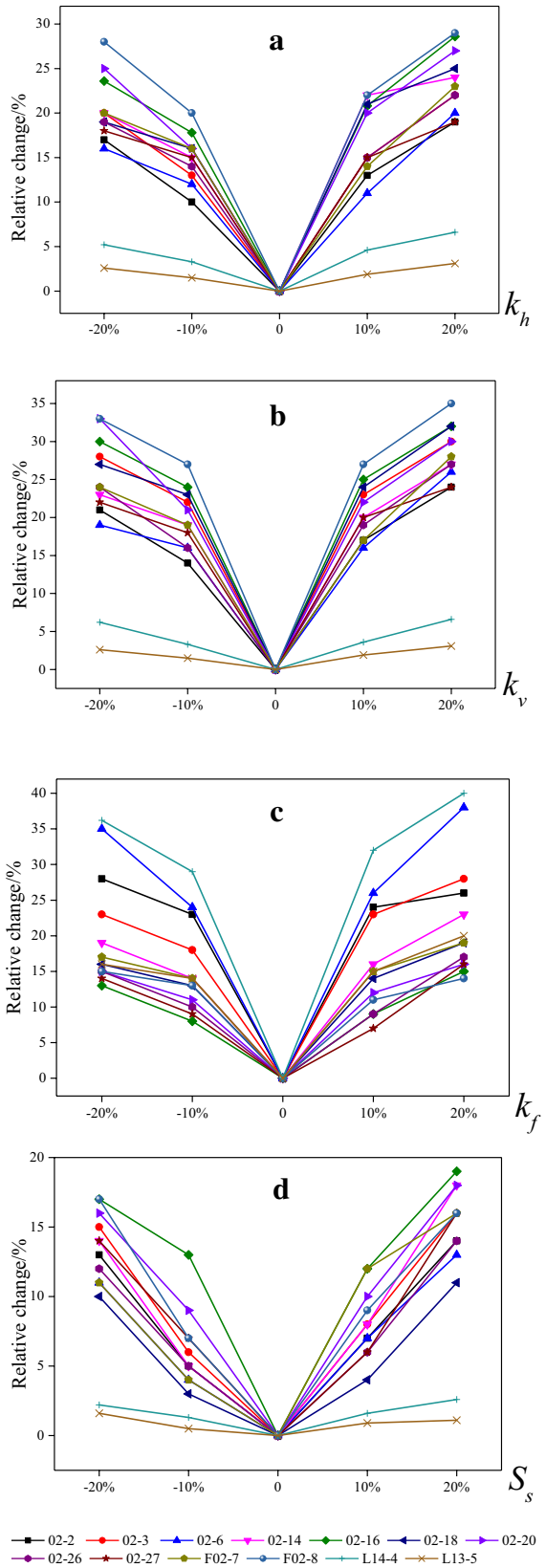

Fig. 6 Sensitivity analysis of main factors: **a** k_h, **b** k_v, **c** k_f, and **d** S_s

supplied by 7 holes. In stage 3, after dewatering for 34 days, 33,180 m^3/day can be supplied by 11 holes. Compared with case 1, case 2 produces a more reasonable amount of water and reaches the safe mining hydraulic pressure more quickly. Thus, it is more feasible than case 1. The model also predicts that there will be the transportation of 2517, 1384, and 6192 m^3 of water between upper aquifers and OLA in stages 1, 2, and 3, respectively. The permeable faults act as the seepage pathway, which is beneficial to the use of OLA water.

Discussion

The good fit of the model was demonstrated from many aspects, such as the relative errors and dynamic change of water level. The initial permeability of faults could not be obtained at this stage due to a lack of special hydrogeological investigation, so initial values were assigned to faults and then corrected to help the calibration. However, the fault was defined as a homogeneous geological body in this paper, and the fitted values do not represent natural vertical variation. Through the sensitivity analysis, we found that the priority sequence of impacts on the predicting results was k_f, k_v, k_h, and S_s. Thus, the permeability of the faults (k_f) was confirmed as the most important factor in sensitivity analysis. The bigger the errors in k_f, the more uncertain the predicted water volume. Compared to case 1 (regional dewatering), case 2 (targeted dewatering) produces a more reasonable amount of water in a practical time frame, so the uncertainty in the case 2 calculations was investigated. Due to the lack of exploration for pervious faults, the value range of k_f was varied from −20% to +20% while other factors were varied from −10% to +10% (Table 4). Under the positive value combination conditions, the water supply from the no. 1, 2, 3 zones were increased by 4040, 4203, and 5161 m^3/day, whereas water supply decreased by 4141, 3972, and 4446 m^3/day under negative combination. Because the faults act as a delivery channel between the upper and the lower aquifers, a change in k_f causes large variations for the predicted response of the L13-5 and L14-4 holes (Fig. 8c). Thus, more investigation of the faults' hydraulic conductivity was recommended. It is interesting that for years, the permeable faults were considered a hazard for mine water control in China (Zhang et al. 2014), they were shown in this analysis to improve the OLA water supply. The existence of impermeable faults causes the available water resource of zone no. 3 in case 2 to be larger than the other zones (Table 3).

The retention of barrier pillars near the permeable faults is significant to both mine safety and water utilization, so this issue needs to be investigated carefully before excavation. The critical water inrush coefficients of 0.1 MPa/m, suitable for

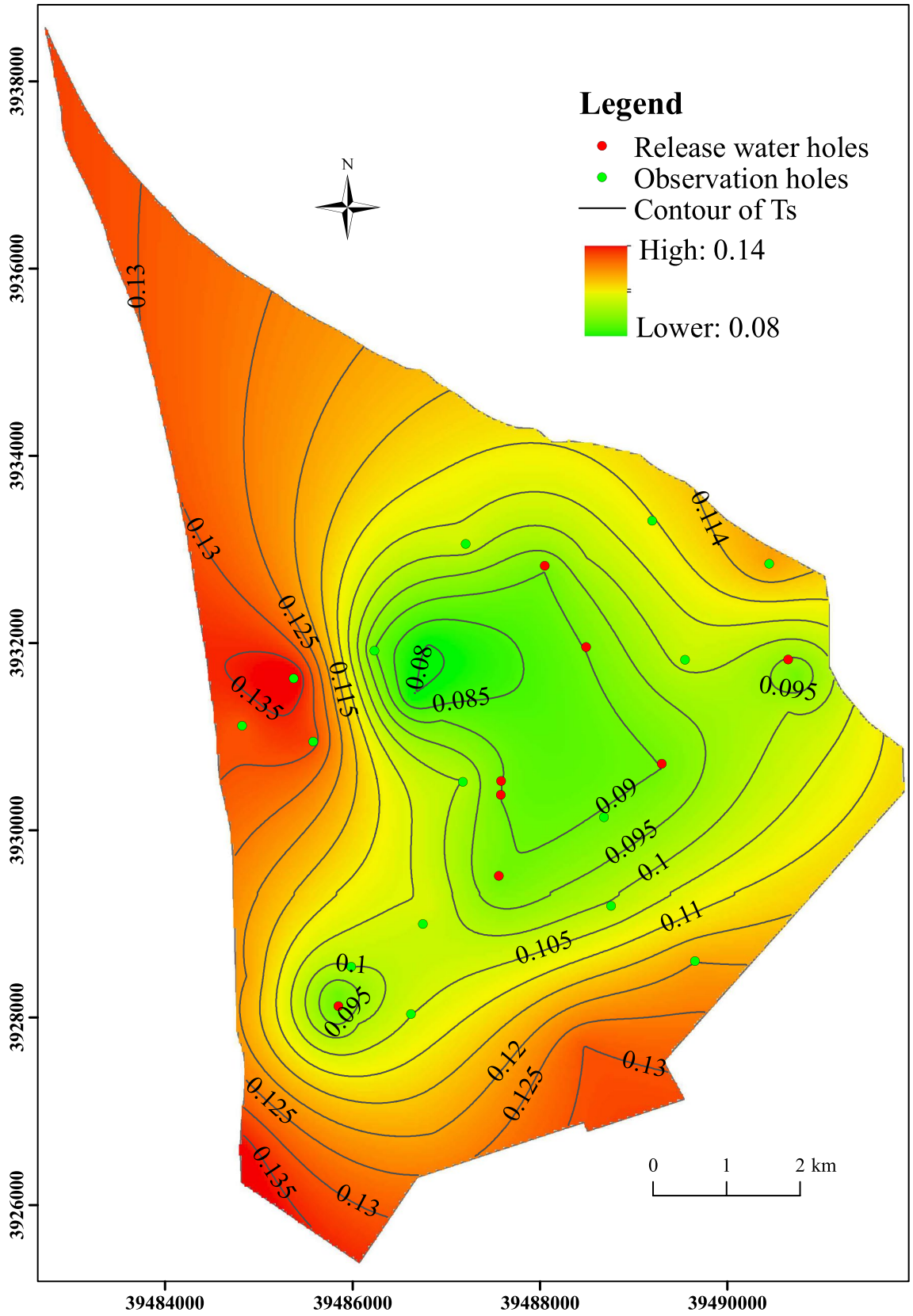

Fig. 7 The *Ts* distribution of case 1

Table 2 Target drawdown (*S*), time (*T*) and volume (*V*) for water release holes in case 1

Holes	*P* (MPa)	M (m)	*Ts* (MPa/m)	*S* (m)	*T* (day)	*V* (m^3/day)
FO2-3a	6.36	48	0.13	150	177	7344
FO2-4a	5.48	35	0.15	189	168	7819
FO2-7	5.5	46	0.12	82	208	6338
FO2-8	5.8	45	0.13	121	173	6715
FO2-10	6.25	43	0.14	190	213	7219
FO2-12	5.83	41	0.14	168	195	6837
FO2-18	5.26	39	0.13	135	184	7352
FO2-19	6.04	48	0.12	122	265	9844

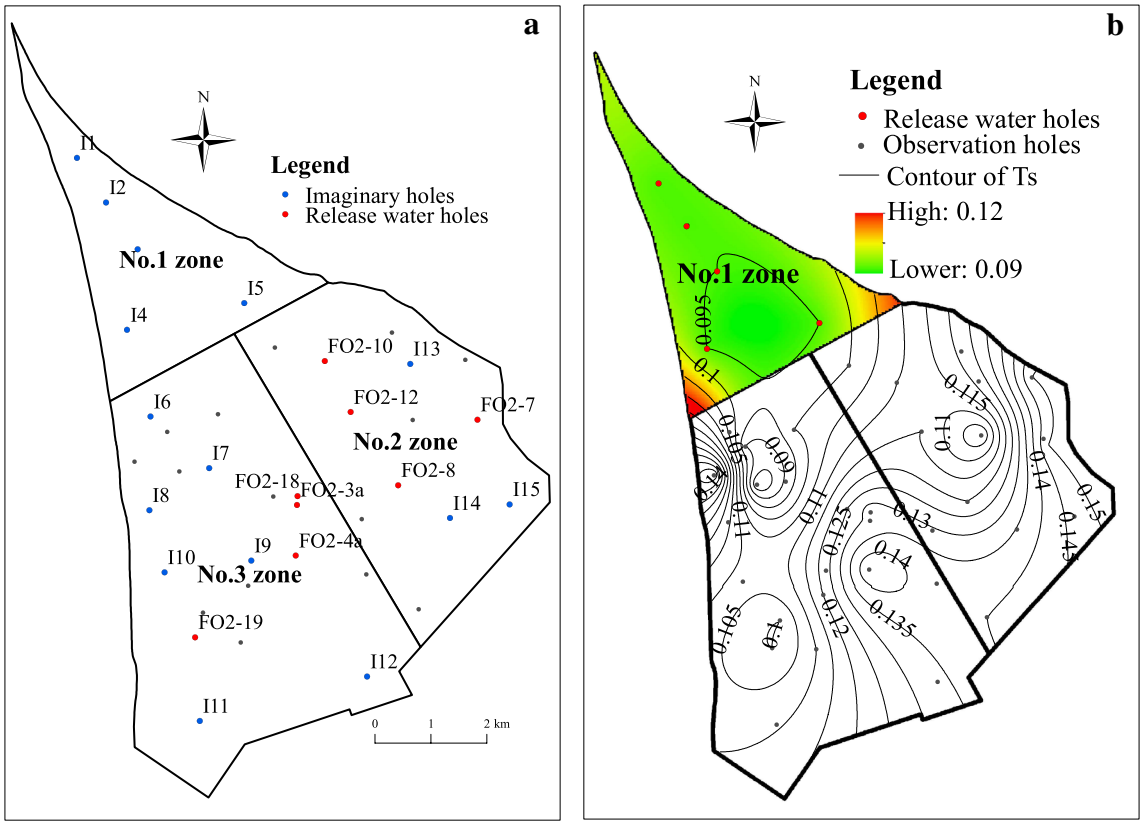

Fig. 8 The *Ts* distribution of case 2: **a** dewatering zoning and proposed drillings, **b** *Ts* distribution of NO. 1 zone, **c** *Ts* distribution of NO. 2 zone, **d** *Ts* distribution of NO. 3 zone

normal conditions, was adopted to calculate the safe dewatering pressure in this paper. This analysis could be refined in the future to satisfy the inrush coefficient of 0.06 MPa/m used for the complex conditions, for localized areas threatened by the strong structural geological movements.

Conclusions

The feasibility of utilizing OLA water from the XCM was used as a case study to resolve conflicts over the use of water resources in north China. A numerical simulation model was established to investigate the balance between

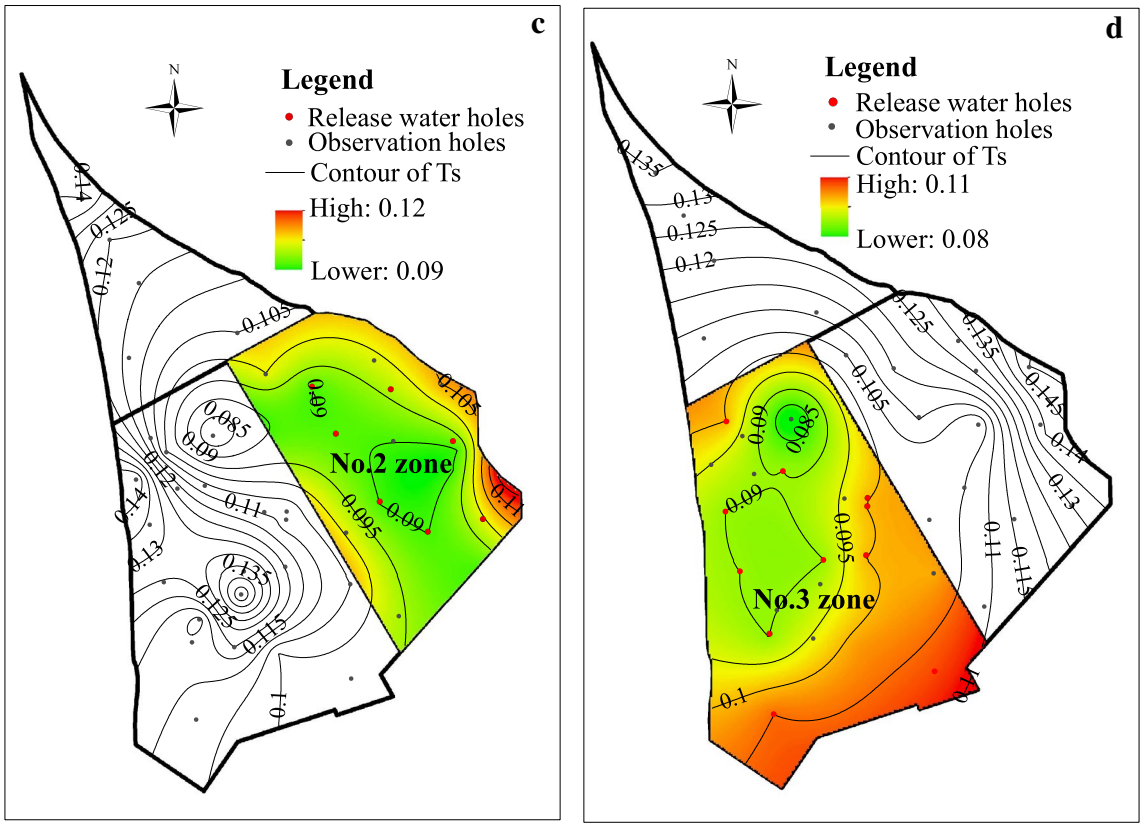

Fig. 8 (continued)

safe mining and reasonable water supply. To reduce water inrush hazards, the drawdown required by dewatering was calculated using conventional floor water inrush assessment formula. Two dewatering plans (regional and local) were proposed to discuss the balance between reasonable water supply and safe mining. After hundreds of trial model runs with varied parameters, fitted hydrogeological parameters were obtained; the final permeability of faults equaled 18 m/day. Comparison between the model outputs and the observed hydraulic head of each hole, and an analysis of the dynamic change of water head confirmed that the calculated values were consistent with the measured values.

Through sensitivity analysis, the parameter k_f (fault permeability) was shown to have more influence than k_h, k_v, and S_s, especially for drill holes near the permeable faults such as O2-2 and O2-6. The results were more sensitive to k_v than to k_h, suggesting that changes in vertical conductivity may induce a longer seepage path than in the horizontal direction. The sensitivity to S_s was the lowest among the four main factors, indicating that the permeability of OLA is high and its lateral recharge may be more significant than the static reserves.

Compared with the regional plan (case 1) that produced surplus mine water, successive local dewatering (case 2), in which the OLA was divided into three zones was recommended. A stable released mine water flow rate (29,119, 29,159, and 33,180 m^3/day for zones 1, 2, and 3, respectively) can be used successively by the GCCE as the corresponding coal seams are mined. Meanwhile, the uncertainty of case 2 was calculated: the water supply of the three zones may increase by 4040, 4203, and 5161 m^3/day or decrease by 4141, 3972, and 4446 m^3/day under the selected range of sensitivity of key parameters.

Although permeable faults were previously treated as a potentially dangerous, we found that the faults can be used to improve water production in this model. As a result, further investigations are suggested for the proposed case, with safety pillars near the faults. The analysis still needs to be improved and refined to reduce possible risks. Nevertheless,

Table 3 Target drawdown (*S*), time (*T*) and volume (*V*) for water release holes in case 2

Stage	Holes	*P* (MPa)	M (m)	*Ts* (MPa/m)	*S* (m)	*R*[a] (MPa)	*T* (day)	*V* (m^3/day)
1	I1	6.46	44	0.14	203	4.42	42	5827
	I2	6.67	46	0.14	203	4.63	44	5793
	I3	5.73	42	0.13	151	4.21	38	5808
	I4	5.74	42	0.13	148	4.25	37	5932
	I5	5.05	44	0.11	57	4.47	28	5759
2	FO2-7	5.5	46	0.12	82	4.67	27	4035
	FO2-8	5.8	45	0.13	121	4.58	30	4173
	FO2-10	6.25	43	0.14	190	4.34	36	4083
	FO2-12	5.83	41	0.14	168	4.14	34	4159
	I13	5.61	42	0.13	135	4.25	32	4168
	I14	5.68	43	0.13	133	4.34	34	4255
	I15	6.37	44	0.14	191	4.45	38	4286
3	FO2-3a	6.36	48	0.13	150	4.86	28	2873
	FO2-4a	5.48	35	0.15	189	3.58	29	2865
	FO2-18	5.26	39	0.13	135	3.9	32	2897
	FO2-19	6.04	48	0.12	122	4.81	34	3073
	I6	5.63	46	0.12	97	4.65	27	2943
	I7	5.08	45	0.11	54	4.53	20	3488
	I8	5.71	43	0.13	134	4.36	31	3278
	I9	5.05	41	0.12	86	4.18	28	2871
	I10	5.15	44	0.11	67	4.47	32	2958
	I11	4.72	42	0.11	50	4.21	24	2961
	I12	5.13	41	0.12	95	4.17	31	2973

[a]*R* is the remaining hydraulic pressure, MPa

Table 4 The uncertain water supply of case 2 induced by the controlling factors

Water supply (m^3/day)	k_f (m/day)		k_v (m/day)		k_h (m/day)		S_s		Total (m^3/day)	
	+20%	−20%	+10%	−10%	+10%	−10%	+10%	−10%		
No. 1 zoning	+1257	−1431	+1125	−1047	+842	−791	+816	−872	+4040	−4141
No. 2 zoning	+826	−1042	+1553	−1281	+1034	−831	+790	−818	+4203	−3972
No. 3 zoning	+1872	−1628	+1418	−1033	+1027	−982	+844	−803	+5161	−4446

+, represents an increase; −, represents a decrease

this study indicates the potential benefit of coordinated utilization of mine water resources.

Acknowledgements Financial support for this work was provided by the Fundamental Research Funds of the State Key Program of National Natural Science of China (No. 41430643), The National Basic Research Program of China (No. 2015CB251601). The authors also thank the reviewers for their useful comments.

References

Abraham MR, Susan TB (2017) Water contamination with heavy metals and trace elements from Kilembe copper mine and tailing sites in Western Uganda: implications for domestic water quality. Chemosphere 169:281–287

Afzal M, Battilani A, Solimando D, Ragab R (2016) Improving water resources management using different irrigation strategies and water qualities: field and modelling study. Agr Water Manage 176:40–54

Bai H, Ma D, Chen Z (2013) Mechanical behavior of groundwater seepage in karst collapse pillars. Eng Geol 164:101–106

Cooper HH, Jacob CE (1946) A generalized graphical method for evaluating formation constants and summarizing well-field history. Eos Trans AGU 27(4):526–534

Dong D, Sun W, Xi S (2012) Optimization of mine drainage capacity using FEFLOW for the no. 14 coal seam of China's Linnancang coal mine. Mine Water Environ 31:353–360

ElZehairy AA, Lubczynski MW, Gurwin J (2018) Interactions of artificial lakes with groundwater applying an integrated MODFLOW solution. Hydrogeol J 26:109–132

Huang F, Wang GH, Yang YY, Wang CB (2014) Overexploitation status of groundwater and induced geological hazards in China. Nat Hazards 73:727–741

Huo A, Peng J, Chen X, Deng L, Wang GL, Cheng YX (2016) Groundwater storage and depletion trends in the Loess areas of China. Environ Earth Sci 75:1167–1178

Islam MB, Firoz ABM, Foglia L, Marandi A, Khan AR, Schüth C, Ribbe L (2017) A regional groundwater-flow model for sustainable groundwater-resource management in the south Asian megacity of Dhaka, Bangladesh. Hydrogeol J 25:617–637

Ji ZK, Zhang Y, Li K (2003) The research of water release experiment in Xinglongzhuang coalmine, Yanzhou mining area. Safe Effic Mining 25(1):364–369 **(in Chinese)**

Kotir JH, Smith C, Brown G, Marshall N, Johnstone R (2016) A system dynamics simulation model for sustainable water resources management and agricultural development in the Volta River Basin, Ghana. Sci Total Environ 573:444–457

Li G, Zhou W (2006) Impact of karst water on coal mining in north China. Environ Geol 49:449–457

Li LC, Yang TH, Liang ZZ, Zhu WC, Tang CA (2011) Numerical investigation of groundwater outbursts near faults in underground coal mines. Int J Coal Geol 85:276–288

Li H, Bai H, Wu J, Zhao HM, Ma K (2017) A method for prevent water inrush from karst collapse column: a case study from Sima mine, China. Environ Earth Sci 76:493–503

Liu QS (2009) A discussion on water inrush coefficient. Coal Geol Explor 37(4):34–37 **(in Chinese)**

Ma QF, Zhong LH (2011) Water discharge numerical simulation of Ordovician Limestone dewatering for lower coal group in no 1 exploration area, Xinglongzhuang coalmine. Coal Geol Chin 23(4):31–36 **(in Chinese)**

Ma D, Bai H, Miao X, Pu H, Jiang BY, Chen ZQ (2016) Compaction and seepage properties of crushed limestone particle mixture: an experimental investigation for Ordovician karst collapse pillar groundwater inrush. Environ Earth Sci 75:11–25

Mahmoudpour M, Khamehchiyan M, Nikudel MR, Ghassemi MR (2016) Numerical simulation and prediction of regional land subsidence caused by groundwater exploitation in the southwest plain of Tehran, Iran. Eng Geol 201:6–28

Ministry of Health (Ministry of Health of the People's Republic of China, Standardization Administration of the People's Republic of China) (2005) The reuse of urban recycling water-water quality standard for industrial uses (GB/T19923-2005). Standards Press of China, Beijing **(in Chinese)**

Motagh M, Shamshiri R, Haghshenas M, Wetzel HU, Akbari B, Nahavandchi H, Roessner S, Arabi S (2017) Quantifying groundwater exploitation induced subsidence in the Rafsanjan plain, southeastern Iran, using InSAR time-series and in situ measurements. Eng Geol 218:134–151

Mu W, Wu Q, Xing Y, Qian C, Wang Y, Du YZ (2018) Using numerical simulation for the prediction of mine dewatering from a karst water system underlying the coal seam in the Yuxian Basin, northern China. Environ Earth Sci 77:215–234

Qiao W, Li WP, Zhang X (2014) Characteristic of water chemistry and hydrodynamics of deep karst and its influence on deep coal mining. Arab J Geosci 7(4):1261–1275

SACMSC (State Administration of Coal Mine Safety of China) (2018) Regulations of mine water disaster prevention. China University of Mining and Technology Press, Xuzhou, pp 31–32 **(in Chinese)**

Singh R, Venkatesh AS, Syed TH, Reddy AGS, Kumar M, Kurakalva RM (2017) Assessment of potentially toxic trace elements contamination in groundwater resources of the coal mining area of the Korba coalfield, central India. Environ Earth Sci 76(16):566

Sun W, Zhou W, Jiao J (2016) Hydrogeological classification and water inrush accidents in China's coal mines. Mine Water Environ 35:214–220

Sun Y, Liu N, Shang J, Zhang JY (2017) Sustainable utilization of water resources in China: a system dynamics model. J Clean Prod 142:613–625

Theis CV (1935) The relation between the lowering of the Piezometric surface and the rate and duration of discharge of a well using groundwater storage. Eos Trans AGU 16(2):519–524

Wang X, Sun L, Wang Z, Liu CL, Zhang Y (2014) An analysis of the resilience capacity of soils in north China: a study on land subsidence treatment. B Eng Geol Environ 73:723–731

Wu Q, Zhou W, Li D, Di ZQ, Miao Y (2006) Management of karst water resources in mining area: dewatering in mines and demand for water supply in the Dongshan mine of Taiyuan, Shanxi Province, north China. Environ Geol 50:1107–1117

Wu Q, Hu BX, Wan L, Zheng CM (2010) Coal mine water management: optimization models and field application in North China. Hydrol Sci J 55:609–623

Wu YX, Shen S, Yuan D (2016) Characteristics of dewatering induced drawdown curve under blocking effect of retaining wall in aquifer. J Hydrol 539:554–566

Xue S, Liu Y, Liu S, Li WP, Wu YL, Pei YB (2018) Numerical simulation for groundwater distribution after mining in Zhuanlongwan mining area based on visual MODFLOW. Environ Earth Sci 77:400–409

Yin S, Zhang J, Liu D (2015) A study of mine water inrushes by measurements of in situ stress and rock failures. Nat Hazards 79:1961–1979

Yin H, Zhou W, LaMoreaux JW (2018) Water inrush conceptual site models for coal mines of China. Environ Earth Sci 77:746–753

Zhang J (2005) Investigations of water inrushes from aquifers under coal seams. Int J Rock Mech Min 42:350–360

Zhang R, Jiang Z, Zhou H, Yang CW, Xiao SJ (2014) Groundwater outbursts from faults above a confined aquifer in the coal mining. Nat Hazards 71:1861–1872

Zhang SC, Yu DL, Li SQ, Wang YJ, Qiao W (2015) Lower group coal seams floor karst water parameter computation and water bursting hazard assessment in Xinglongzhuang coalmine, Yanzhou mining area. Coal Geol China 27(3):35–39 **(in Chinese)**

Zhu WC, Wei CH (2011) Numerical simulation on mining-induced water inrushes related to geologic structures using a damage-based hydromechanical model. Environ Earth Sci 62:43–54